Moisture migration during loading and shearing of unsaturated sand

Bestun Shwan[a]

Department of civil and structural engineering, University of Sheffield, Mappin Building Street, Sheffield S1 3JD, UK.

Abstract. A series of drained unsaturated direct shear tests were conducted on a fine sand where suction was controlled by means of a hanging water column. A rise in the water level in the column was observed in conjunction with normal stress application for unsaturated samples. During shearing, the water level in the column also increased indicating continued water content loss from the sand. This is over and above any change in saturation that would arise due to volume change. Samples taken after the test for water content measurement confirmed the observed effect. Discussion of the phenomenon in the context of the soil water characteristic curve (SWCC) is presented and a simple hypothesis to explain this behaviour is proposed.

1 Introduction

The arrangement of water within the voids has a significant effect on the behaviour of unsaturated soils, [1] and [2]. Wheeler [3] defined two different forms of liquid water in unsaturated soil: bulk and meniscus water. Soil follows the bulk water form for any suction values less than the air entry value. The meniscus water form, however, is more pronounced when the applied suctions are greater than the air entry value, [2].

Understanding these two liquid forms during shearing and their effects on the behaviour of the unsaturated soil is significant. Romero and Vaunat [4] studied the soil water characteristic curve (SWCC) for deformable clays following which delimiting zones in the water retention curve were defined, which are controlled by water ratio (volume of water to volume of solids). Two zones: intra-aggregate water (adsorbed water) and inter-aggregate water were recognized. In the latter zone, air is occluded and the water ratio is highly sensitive to the mechanical effects.

The hydro-mechanical behaviour of unsaturated soils has been investigated in terms of the SWCC. Generally, the most recent studies of the SWCCs emphasised the cyclic drying and wetting behaviours. The cyclic behaviours were studied (for example, [5-6]) in terms of scanning path which can be defined as any intermediate point between the main drying and wetting curves, [6]. The effect of dilation during shearing on the drying behaviour and its consequence on the SWCC in a controlled suction test, however, is limited.

This paper presents, therefore, work in progress that investigates the drying behaviour during shearing at a low range of suctions for unsaturated sand in a context of the SWCC using a modified direct shear apparatus. The effect of the mechanical straining in a context of the SWCC on the basis of the experimental results performed in this study is also addressed qualitatively.

2 Experimental work

2.1 Soil properties and SWCC

A commercial fine sand, designated fraction D by the supplier- available from the David Ball Group-UK, was used. The physical properties for the sand are shown in Table 1.

Table 1. Physical properties for the test dry sand.

Gs	γ_{sat_3} kN/m	γ_{dry_3} kN/m	e	Particle range mm	Relative Density %
2.65	19.33	15.3	0.70	0.075-0.3	52

The SWCC was obtained using two different methods, the filter paper and hanging column technique (HCT) as shown in Fig. 1. For the HCT, a bespoke circular shear box of diameter 80 mm was used with additional features over standard laboratory shear boxes to be adaptable for the unsaturated experiments, see Fig. 2a. Suction was controlled by means of a hanging water column (burette) as shown in Fig. 2b. The SWCC was determined at null load condition. More details with regards to sample preparation and suction application is given by [7].

[a] bjnshwan@gmail.com

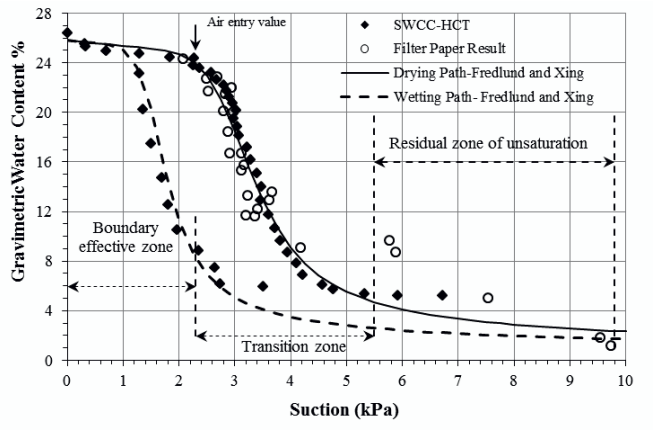

Figure 1. SWCC using the HCT and filter paper method.

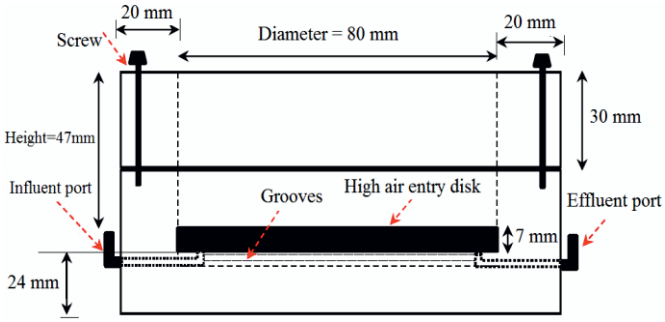

(a)

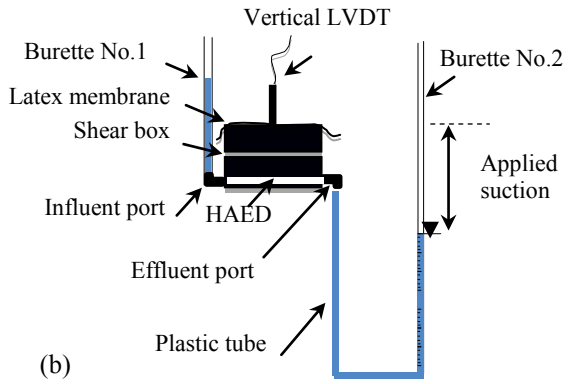

(b)

Figure 2. (a) Modified direct shear box (b) suction application using the HCT and filter paper method.

2.2 Moisture migration during loading and shearing

A series of drained direct shear tests were conducted on unsaturated sand at three normal stresses: 50, 100 and 200 kPa and at a range of nominal suctions: 2, 4 and 6 kPa where the movement of water was observed immediately after the normal stress application. The stated suction head measured at the soil surface was the distance from the water level in the burette to the soil surface. The applied suction was selected according to the SWCC for the sand used. Values of 2 and 6 kPa nominal suction were selected since they are close to the air entry suction and residual suction for the sand used, see Fig. 1. Finally, to investigate the behaviour of unsaturated sand at the transition zone (zone between air entry and residual suctions - see Fig. 1), a value of 4 kPa nominal suction was also utilised. Table 2 shows the nominal and suction values before and after the normal stress application for σ = 50 kPa for three repeat tests denoted as 1, 2 and 3 in Table 2. The water migration after normal stress application for σ = 100 and 200 kPa was identical with that obtained for σ = 50 kPa, however, only data for σ = 50 are presented. The idiom suction denotes the nominal suction value in the context of this paper and in the figure's legends.

During shearing, the water level in the burette also increased indicating continued water content loss from the sand.

Table 2. Nominal and suction values before and after application of the normal stress for σ = 50 kPa.

σ (kPa)	$s_{nominal}$ (kPa)	s_{before} (kPa)	s_{after} (kPa)
50-1	2	2.17	2.06
50-2	2	2.06	2.04
50-3	2	2.19	2.18
50-1	4	4.35	4.27
50-2	4	4.1	4.1
50-3	4	3.95	3.89
50-1	6	5.33	5.32
50-2	6	5.88	5.79
50-3	6	6.02	5.92

2.3 Determination of the Scanning path

The scanning path is a consequence of the suction change to a lower value. To determine the start of the scanning path on the main drying curve (point A in Fig. 2a), weight volume relationships were used. Prior to the test, the amount of water extracted from the sample by lowering the burette to apply a specific suction was collected in a container (water was expelled from an open-ended burette using a syringe) and measured to a scale of three decimal place accuracy and hence total weight of the sample was adjusted accordingly. Subsequently, the total unit weight of the sample (γ_t) at a known initial volume was calculated using the equation:

$$\gamma_t = \frac{W_t}{V_t} \quad (1)$$

where W_t is the total weight (kN) and V_t is the total volume (m^3). Degree of saturation (S_r) and water content (w) were calculated as follows:

$$S_r = \frac{\gamma_t (1+e) - G_s \gamma_w}{e \gamma_w} \quad (2)$$

$$w = \frac{S_r e}{G_s} \quad (3)$$

where e is the initial void ratio (= 0.7- see Table 1), G_s is the specific gravity and γ_w is the unit weight of water (kN/m^3). Suction head was measured as a distance from water level in the burette to the soil surface. By knowing the water content and suction value after

application of the normal stress prior to the test, the start point of the scanning path on the main drying curve (point A in Fig. 2a) can be located.

At the end of the test, 5 samples were taken along height (47mm) of the sample to track the moisture content loss. The suction head for sample No. 1 (the samples were numbered from the top to bottom) was determined according to the last water level in the burette which was captured by a camera, installed in front of the burette during the test to take an image for the water level in the burette every 30 minutes. Suction head for sample No. 2 was less than the suction head of sample No. 1 by (47/5) mm. This calculation was replicated for other samples (i.e. samples No. 3, 4 and 5). By knowing both suction and water content, the end of the scanning path was determined. The measured water content was also compared with the calculated water content which was determined at different stages of the test using Eqs. 1, 2 and 3. Following this the calculated water content was paired with the inferred suction (obtained based on water level in the burette captured by the camera at different stages during the test) and plotted on the SWCC (see Fig. 2a-hollow triangle symbol). The calculation was based on adjusted height of the sample during shearing (compressibility and dilation behaviours) and unit weight. The height of the sample during shearing was obtained from a vertical LVDT reading. Then, void ratio was determined according to the adjusted total volume as follows:

$$V_v = V_t - V_s \tag{4}$$

$$e = \frac{V_v}{V_s} \tag{5}$$

where V_v is the volume of voids and V_s is the volume of solid.

3 Results

3.1 Drying behaviour during shearing at different low suctions and constant normal stress

Figures 3, 4 and 5 plot the gravimetric water content versus suction at constant σ = 50 kPa and different suctions of 2, 4 and 6 kPa showing the scanning paths. The start of the scanning path (point A in Fig. 3a) is plotted based on the adjusted values of the suction after the application of the normal stress (see Table 2). The beginning of the scanning path for a few cases was observed either above or below the drying path of SWCC-HCT (e.g. see Fig. 4a - circled). This was attributed to the effect of void ratio in which the sample initially was deemed to be looser (above the SWCC-HCT curve) or denser (below the SWCC-HCT curve). The denser sample provided a smaller void ratio and hence less water was retained between the voids.

In Figs. 3, 4 and 5, the most significant drying behaviour (water migration) occurred to the sample No. 1 (solid circle). The overall trend showed the drying behaviour at the different suction levels with a few cases of the wetting near the failure plane (e.g. see solid square-Fig. 3a).

The drying behaviour is attributed to (i) the effect of the normal stress application which caused water movement downwards and (ii) due to concentration of the suction in the shearing zone but not the entire thickness of the sample. This caused water migration into or out of the shearing zone. This may indicate why the wetting behaviour for most of the cases was observed near the failure plane (solid square in Fig. 3a - near the failure plane).

Concentration of the suction is due to the dilative behaviour in which dilation created bigger voids between the particles near the shear band for water to move into. The dilative behaviour was also observed for the unsaturated samples prepared at normal stresses of 100 and 200 kPa, detailed in [7].

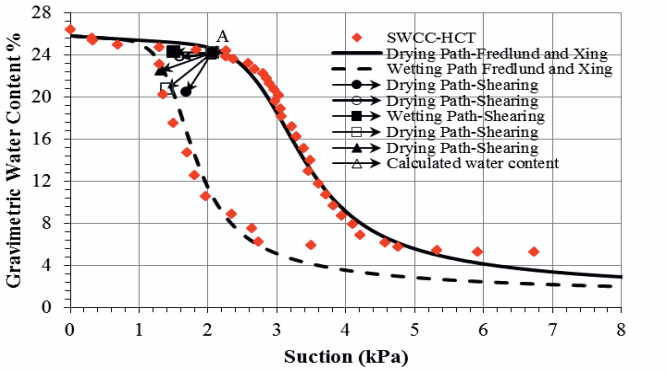

(a)

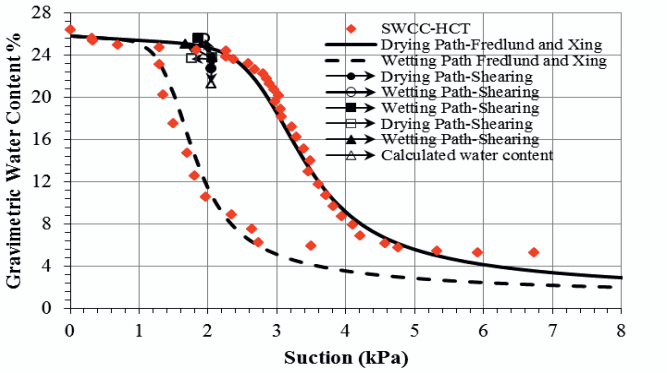

(b)

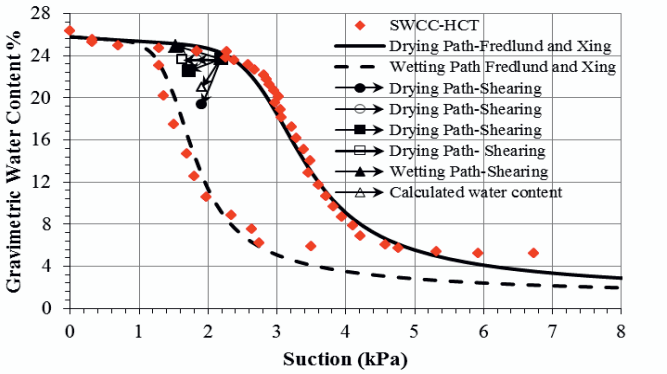

(c)

Figure 3. Scanning path for σ = 50 kPa and s = 2 kPa for (a) first test-1 (b) second test-2 (c) third test-3.

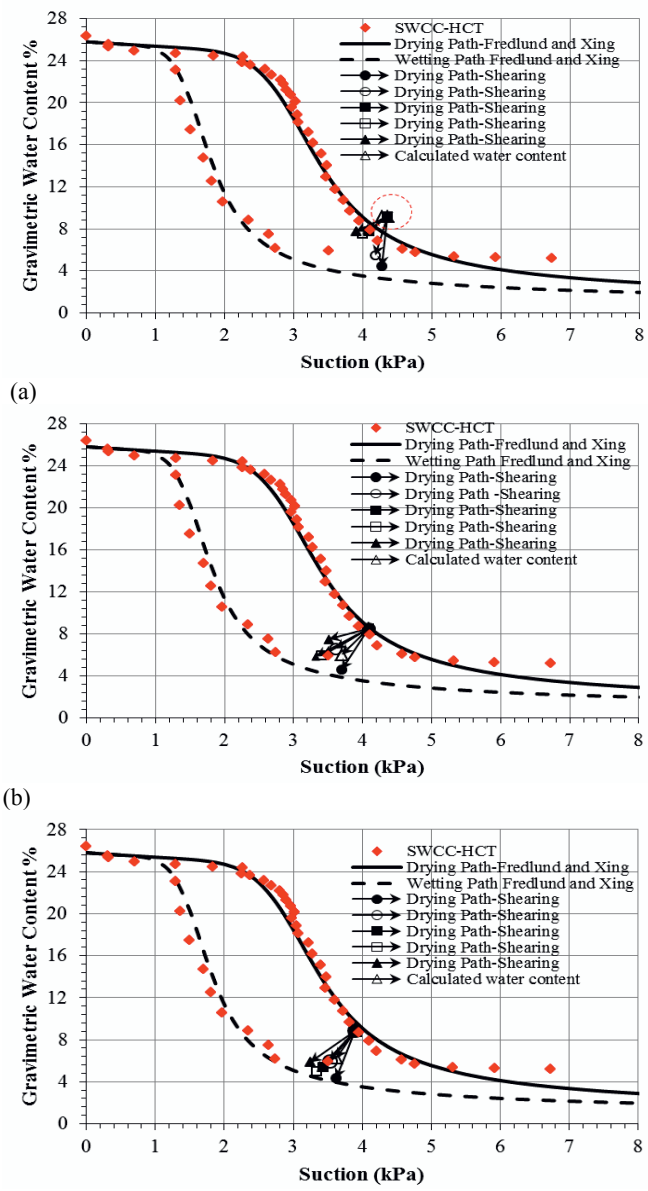

Figure 4. Scanning path for $\sigma = 50$ kPa and $s = 4$ kPa for (a) first test-1 (b) second test-2 (c) third test-3.

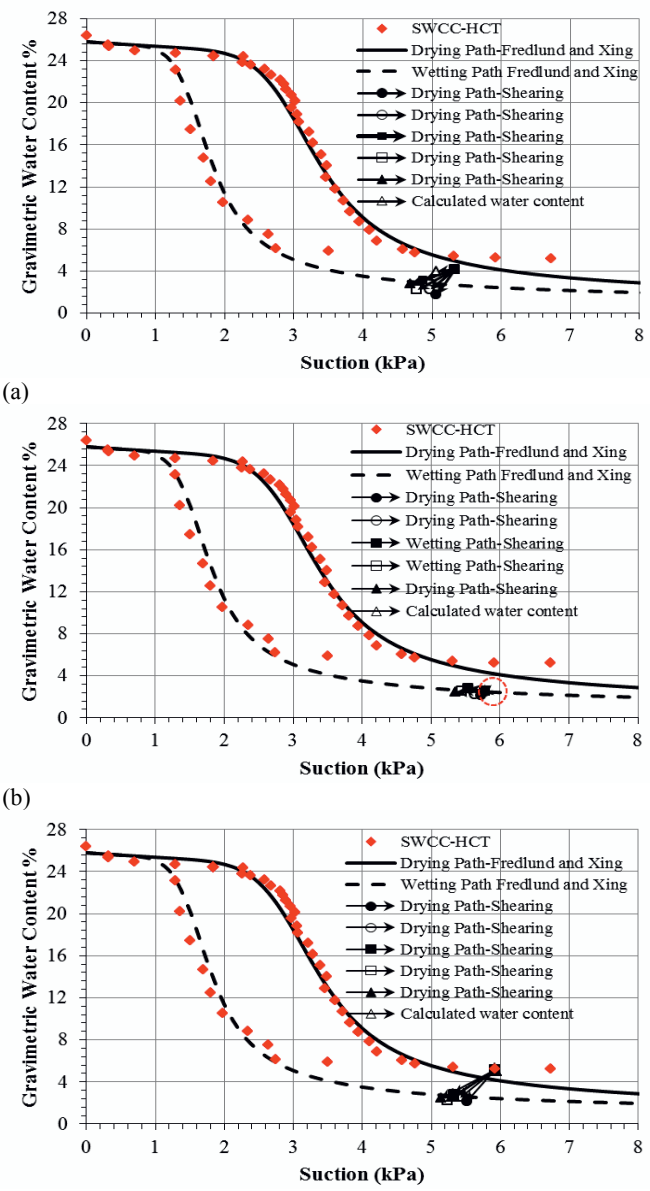

Figure 5. Scanning path for $\sigma = 50$ kPa and $s = 6$ kPa for (a) first test-1 (b) second test-2 (c) third test-3.

4 Discussion

The water level in the burette was seen to rise in conjunction with the normal stress application. During shearing, the water level in the burette also increased indicating continued water content loss from the samples. This was over and above any change in saturation that would arise due to volume change. Discussion of the phenomenon in the context of the SWCC is presented and a simple hypothesis to explain this behaviour is proposed.

The sample's paths on the SWCC in Figs. 3 to 5 typically showed drying behaviour with only a few wetting cases. The wetting path A to B in Fig. 6 is the expected behaviour which is attributed to an increase of degree of saturation during shearing (due to decrease in void ratio) and hence in suction. The wetting path is studied broadly in the field of unsaturated soil mechanics.

Although unexpected the drying path A to C in Fig. 6, on the other hand, corresponds to the observed increase in water level in the burette during shearing. As water is expelled from the sample towards the burette during shearing (S_r decreased), the distance from the water level in the burette to the sample surface decreased (s decreased). This means both S_r and s decreased when water is expelled from the sample. A similar situation occurs when water is imbibed by the sample during shearing (both S_r and s increased).

In general, drying behaviour was observed for most samples regardless of whether the samples follow path A to C or A to E. These paths are described in more detail below:

1. Scenario I- path A to C

The drying behaviour on the SWCC in Figs. 3 to 5 was analysed based on this scenario due to the assumed direct relationship between s and S_r.

2. Scenario II- path A to D

If suction is assumed to be constant during shearing (omitting the water level change in the burette), the sample will follow path A to D during drying. However, this scenario is unlikely to occur because suction will change with any change of degree of saturation.

3. Scenario III- path A to E

This scenario is the most likely case to be followed by the sample during drying. Here, the actual measurement of the suction, for example using tensiometers placed into the sample, is required.

The importance of studying the drying behaviour on the SWCC for the Scenario-III is highlighted in that such findings are not reported in the literature yet. The discussion in the next paragraphs is, therefore, devoted to the main affecting factors on the drying path in the context of the SWCC.

It is hypothesised that the drying behaviour is a normal stress and void ratio dependant. In terms of the former, water migration was observed both (i) immediately after the load application and (ii) during shearing. In terms of the latter, suction increased due to the dilative behaviour observed for the most unsaturated samples. The increase of suction caused a decrease in degree of saturation in which this decrease was reversible (dSr_e) and irreversible (dSr_p) change, where the subscripts e and p denote elastic and plastic components. The elastic (dSr_e) and plastic (dSr_p) changes of S_r are a combination of the mechanical process of straining of the soil skeleton under changes of applied stresses (see Fig. 7) and the hydraulic process of water inflow and outflow to individual voids (see Fig. 8).

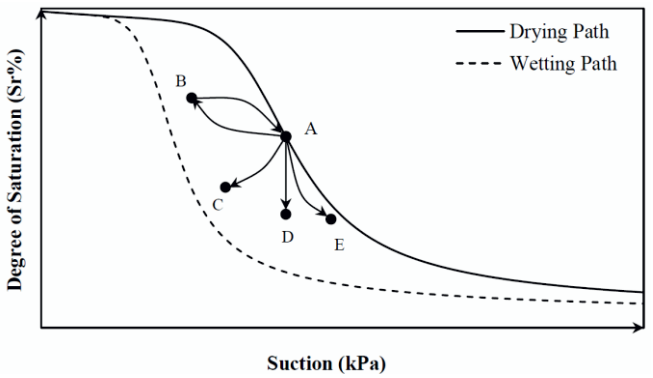

Figure 6. Typical SWCC showing scanning paths.

The elastic change (dSr_e) due to change of the normal stress is attributed to the soil particles and packet elastic deformations, [9]. The (dSr_e) due to the hydraulic process, however, is attributed to a change of radius of the meniscus, from position 2 to 3 in Fig. 8, and a contact angle.

The plastic change (dSr_p) due to the mechanical process, on the other hand, is because of slippage at inter-particle contacts which is controlled by the normal components of the contact forces (see Fig. 7b). The hydraulic effect on the (dSr_p) is due to further change of meniscus radius (position 3 to 4 in Fig. 8) in which air can break through into the voids.

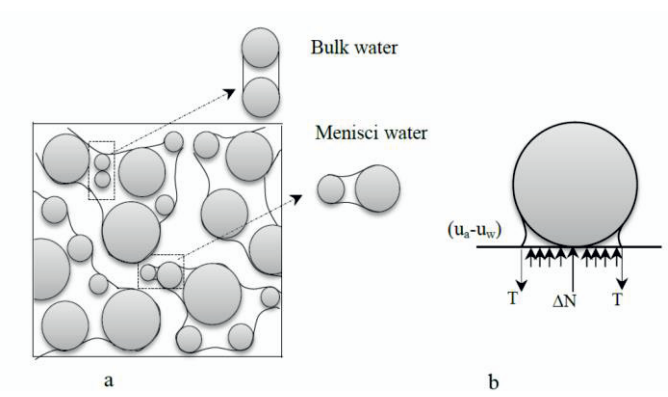

Figure 7. (a) Bulk and menisci water forms (b) Distribution of forces between two solid spheres, after [11].

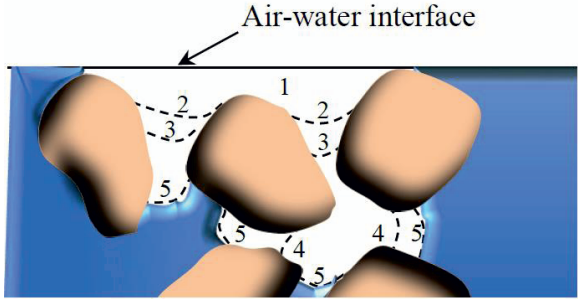

Figure 8. Air-water interface at different suctions, after [10].

5. Conclusions

1. A series of drained direct shear tests were conducted on unsaturated sand at a range of low suctions where the movement of water (drying) was observed immediately after the normal stress application and during shearing.
2. The drying behaviour was discussed in the context of the SWCC and a simple hypothesis was proposed which included the main factors affecting the water migration. It was hypothesised that the drying behaviour was attributed to the effects of the normal stress and dilative behaviour.

Acknowledgments

The author wishes to acknowledge the financial support which was provided by the Ministry of Higher Education-Kurdistan (Iraq) for this work.

References

1. S.J. Wheeler, D. Karube, *State of the art report: constitutive modeling*, in Proc. 1st Int. Conf. on Unsat. Soils, Paris pp. 1323-1356, (1995).
2. R. Vassallo, C. Mancuso, *Soil behavior in the small and the large strain range under controlled suction conditions*, in Int. Wksp on Unsat. Soils-Trento, Italy, pp. 10-12, (2000).
3. S.J. Wheeler, *Constitutive modelling of unsaturated soils*, in 4th Int. Conf. on Unsat. Soils, Arizona, USA, (2006).
4. E. Romero, J. Vaunat, *Retention curves of deformable clays*. In: Tarantino, A., Mancuso, C. (Eds.), Exp. Evid. and Theo. App. in Unsat. Soils, Balkema, Rotterdam, pp. 91-106, (2000).
5. D. Gallipoli, S.J. Wheeler, and M. Karstunen, *Modelling the variation of degree of saturation in a deformable unsaturated soil*. Ge'ot. J., **53**(1): pp 105-112, (2003).
6. M. Nuth, L. Laloui, *Advances in modelling hysteretic water retention curve in deformable soils*. Comp. and Geots. J., **35**(6), pp. 835-844, (2008).
7. B.J. Shwan, C. C. Smith, *Increase of the shear strength parameters for unsaturated sand*. Ge'ot. J., (2016), (to be published).
8. B.J. Shwan, C. C. Smith, *Effect of dilation on the degree of saturation at during shear*. Ge'ot. J. , 2016 (to be published).
9. S.J. Wheeler, R.S. Sharma, and M.S.R. Buisson, *Coupling of hydrulic hysteresis and stress-strain behaviour in unsaturated soils*. Ge'ot. J., **53**(1), pp 41-54, (2003).
10. R.A. Fisher, *On the capillary forces in an ideal soil*. Agric. Scie. J., **16**: pp 492-505, (1926).
11. E.C. Childs, *An introduction to the physical basis of soil water phenomena*. London/; Wiley-Interscience, (1969).